ELSEVIER

Sensors and Actuators B 60 (1999) 27–34

SENSORS AND ACTUATORS B CHEMICAL

www.elsevier.nl/locate/sensorb

Pd-coated elastooptic fiber optic Bragg grating sensors for multiplexed hydrogen sensing

Boonsong Sutapun [a], Massood Tabib-Azar [a,b,*], Alex Kazemi [c]

[a] *Electrical Engineering and Computer Science Departments, Case Western Reserve University, Cleveland, OH 44106, USA*
[b] *Macromolecular Science and Physics Departments, Case Western Reserve University, Cleveland, OH 44106, USA*
[c] *Boeing, Space and Defense System, EELV / Delta IV-CBC, 5301 Bolsa Ave., Huntington Beach, CA 92647, USA*

Received 16 February 1999; received in revised form 25 June 1999; accepted 25 June 1999

Abstract

We report a new type of optical hydrogen sensor with a fiber optic Bragg grating (FBG) coated with palladium thin film. The sensing mechanism in this device is based on mechanical stress that is induced in the palladium coating when it absorbs hydrogen. The stress in the palladium coating stretches and shifts the Bragg wavelength of the FBG. Using FBGs with different wavelengths many such hydrogen sensors can be multiplexed on a single optical fiber. Here multiplexing two sensors is demonstrated. Moreover, hydrogen and thermal sensitivities of the sensors were calculated using a simple elastic model. Additionally, to quantify the amount of stress in the palladium film as a function of hydrogen concentration, a novel and very sensitive method was devised and used to detect deflections in a Pd-coated cantilever using an evanescent microwave probe. This stress was in the range of $5.26–8.59 \times 10^{-7}$ Pa for H_2 concentrations of 0.5–1.4% at room temperature, which is about three times larger than that found in the bulk palladium for the same range of H_2 concentrations.

Keywords: Optical sensors; Hydrogen detection; Multiplexed fiber optic sensors; Elastooptic effects; Evanescent microwave

1. Introduction

Fiber optic gas and chemical sensors have been around for many years and various active and passive optical sensors have been designed and constructed to detect hazardous and other gases and chemicals in the past [1–3]. One of the important characteristics of fiber optic sensors is their ability to operate in potentially explosive environments. They have other important characteristics such as simplicity of design and higher sensitivity as well.

Many different types of fiber-optic hydrogen gas sensors have been reported in the past [4–6]. Of the fiber-optic hydrogen sensors reported so far in the literature, the micromirror sensor [4,5] is probably the most well developed one. Almost invariably these sensors as well as the electrical hydrogen sensors use palladium (Pd) as the gas-sensitive layer that when exposed to hydrogen its electrical and optical properties change. The micromirror sensor's structure is quite simple. It consists of a thin film of palladium evaporated at the cleaved end of a multimode fiber optic. Although, the micromirror sensor is simple and inexpensive, its multiplexing capability is quite limited and needs optical switches for re-routing and addressing the sensors.

Butler and Ginley [6] recognized the change in the elastic property of Pd during H_2 absorption and invented the fiber optic sensor based on this property. In their work, the sensor was an interferometer in which one arm (i.e., sensing structure) was coated with a palladium film. In their interferometer, the optical path length of the sensing arm changes as it is exposed to hydrogen or as its temperature is changed. The change in the optical path length shifts the fringes at the output of the interferometer and, hence, it can be detected. This sensor is quite complex and offers no multiplexing capability.

Fiber optic Bragg gratings (FBGs) are simple and intrinsic elements that can be written into a silica fiber using a UV light. FBG sensors have all the advantages of the fiber optic sensors. In addition, these sensors have a built-in self-referencing capability and can be multiplexed along a single fiber. Most of the FBG-based sensors

* Corresponding author. Department of Electrical Engineering and Computer Science, Case Western Reserve University, 10900 Eculid Avenue, Cleveland, OH 44106, USA. Tel.: +1-216-368-6431; fax: +1-216-368-6039; E-mail: mxt@po.cwru.edu

0925-4005/99/$ - see front matter
PII: S0925-4005(99)00240-3

reported in the literature are designed for strain and temperature measurements [7–10]. These sensors are designed for distributed embedded structural strain sensing in bridges, roads, ships and buildings, etc.

Chemical fiber optic sensors are also extensively developed. Both passive and active fiber optic chemical sensors are reported in the literature. The challenge, however, is to design and implement multiplexed chemical sensors on FBGs with good reproducibility, long lifetime, acceptable drift, and good sensitivity. The FBG-based chemical sensors could offer several advantages including self-referencing, multiplexing, electrical isolation, small size, and lightweight.

FBGs are well known and they consist of a single mode fiber core region with a periodically modulated refractive index. In most cases, the FBG acts as a notch filter and reflects the light having a wavelength equal to the Bragg grating wavelength (λ_B). The Bragg wavelength of the grating is given by the expression:

$$\lambda_B = 2 n_{eff} \Lambda \quad (1)$$

where Λ is the period of the index modulation and n_{eff} is the effective refractive index of the fiber.

The basic configuration of the sensor is shown in Fig. 1. The device consists of a Pd-coated FBG. The residual stress that is induced in the Pd film during hydrogen absorption depends on the hydrogen concentration. When the FBG is coated with Pd, the stress associated with the hydrogen absorption in the film can be determined by monitoring the transmission or reflection spectra of the FBG. This is the simplest method of constructing wavelength-multiplexed sensors.

Pd is known for its ability to absorb hydrogen several times that of its own volume. As the Pd film absorbs hydrogen it expands because hydrogen absorption converts Pd to PdH_x which has a lower density and larger volume. When Pd coating on a FBG absorbs hydrogen, mechanical expansion that occurs in the Pd film physically stretches the fiber and causes the grating period, Λ, to expand. This process also changes the grating's refractive index through the elastooptic effect. Due to the fact that the stress (or strain) induced by the formation of the hydride phase depends on the hydrogen gas concentration, the amount of the Bragg wavelength shift can be directly related to the hydrogen gas concentration. As a result, the location of the Bragg wavelength can be used directly to determine the H_2 concentrations.

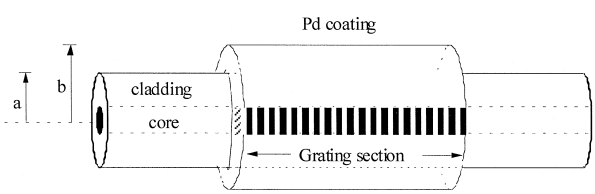

Fig. 1. Schematic diagram of the Pd-coated FBG hydrogen gas sensor.

In our work, a fiber-optic spectrometer with an operating wavelength 800–1000 nm and the FBGs with 0.1–0.4 nm halfwidths were used. For sensors having nominal working range of 2 nm, 100 sensors can then the multiplexed using our network.

The main objective of our work was to design and fabricate FBG-based sensors for hydrogen gas leak sensing to be used in rocket fuel tanks. It is projected that as many as a few hundred cargo-carrying rockets will be deployed per year during the next few decades to launch various communication and reconnaissance satellites into space. To reduce risk and ensure safety of these operations, hydrogen leaks should be detected and prevented; especially before and during their launch while they are in the ambient of the earth atmosphere. We also measured the stress that is induced in a Pd film as a function of hydrogen concentration by using a novel evanescent microwave probe (EMP). The results from the stress measurements were later on used for modeling the sensor response to hydrogen. To the best of our knowledge, the work discussed here is the first report of elastooptic Pd-coated FBG hydrogen sensors. Currently we are expanding our studies to design and fabricate oxygen sensors as well.

2. Experimental procedure

2.1. Sensor fabrication

The FBGs used in our experiments were fabricated on a single mode 125-μm fiber with 5–10 μm diameter core region. The grating reflectivity was 60–99% at λ_B and the grating length was 2–3 cm. An acrylate protective coating on the grating section was removed by using chloroform and cleaned with acetone. Fibers, after etching, with 30–60 μm diameters were found to give good results and they were still easy to handle. To obtain these fibers, the starting 125 μm fibers were etched for 20–25 min in 49% HF solution. The etched fibers then were coated with Pd using an evaporator. The Pd film thickness was monitored during the deposition by using a conventional quartz-crystal thickness monitor. Residual stress after the film deposition was observed and caused the Bragg wavelengths of the FBGs to shift.

2.2. Experimental set-up

The basic apparatus used in our experiments is shown in Fig. 2. Light from a tungsten lamp (broadband source) was injected into the fiber having two FBGs with Bragg wavelengths of 829.73 and 846.65 nm. Both sensors were jointed together using a mechanical splice. Light from the FBG's output was connect to the input of a CCD-based fiber optic spectrometer (OceanOptics S-2000) via a SMA

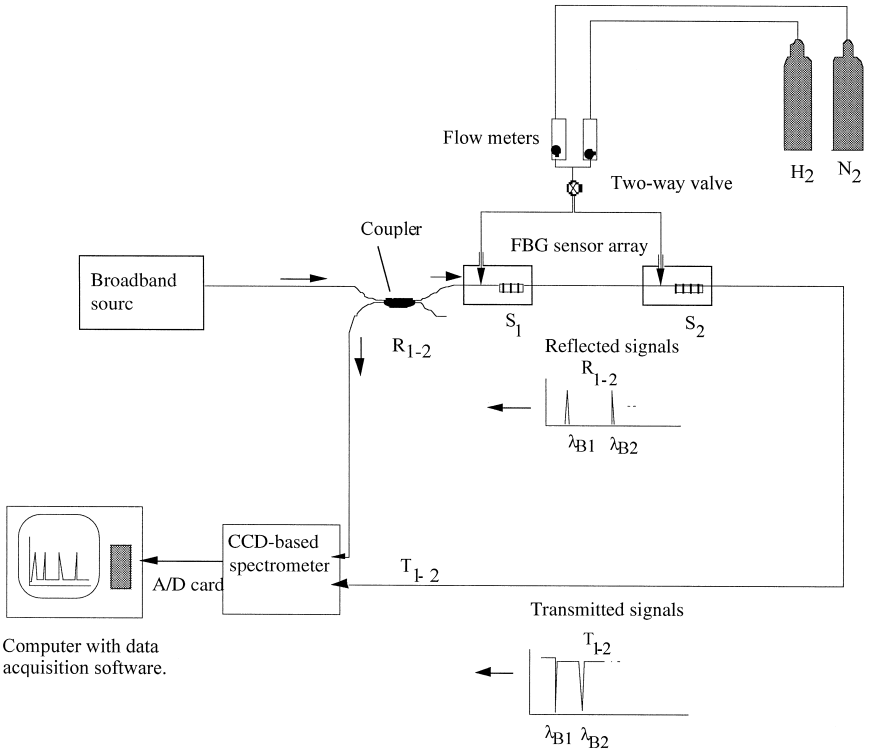

Fig. 2. Experimental set-up used to measure the FBG sensor's response to hydrogen.

connector. The spectrometer had operating range from 800 to 1000 nm and resolution of 0.14 nm/pixel. The sensors were inserted into the gas cells through a rubber cork. The gas cells were made from Teflon tube and had two ports to allow the gas mixture to flow in and out. The dead volume, which included gas cells and carrying gas tubes, was approximately 300 cm^3. The experiments were performed using a mixture of ultra-high purity hydrogen (99.99%) and nitrogen (99.98%). Gas flow rates were measured and controlled individually by a flow meter. All experiments were performed at room temperature and at atmospheric pressure.

The resolution of the spectrometer used in our experiments was roughly 0.14 nm in the 800–1000 nm range. This resolution was not adequate to directly monitor and detect the Bragg wavelength shifts, which were less than 0.1 nm in most of the sensors examined here. To overcome this problem, a spline-fitting routine was applied to the data acquired from the spectrometer.

2.3. Stress measurement in a Pd thin film

Stress in Pd films was quantitatively measured by using the apparatus shown in Fig. 3. A Pd-coated glass cantilever beam was mounted onto a solid support. When exposed to hydrogen, the Pd coating expands and causes the glass cantilever beam to bend downward. The amount of the beam's deflection could be accurately measured and used to calculate the film stress and, hence, to calculate the hydrogen concentration. We used a novel EMP and a fiber optic probe to measure the beam deflection. The EMP has been used extensively for non-destructive characterization of materials [11]. Here, the probe was used as a displacement sensor. Details of the probe set-up have been published elsewhere [11].

EMP principles of operation are explained using a microstripline resonator geometry shown in Fig. 3a. When an object is placed in the vicinity of the tip of the resonator (Fig. 3a), the resonator's reflection coefficient changes as shown in Fig. 3b. Both the resonance frequency (f_r) and the quality factor of the resonator (Q) are affected by the presence of the sample. The amount of change in the resonance (Δf_r and ΔQ) depends primarily on the microwave properties of the sample as well as on the distance between the resonator's tip and the sample (d_s), and on the tip's effective area (A_{eff}).

Microwave properties of a material are a function of permittivity, permeability, and free carrier concentration. These parameters along with density variations, which affect the permittivity, can be mapped using EMP. Different signal detection methods can be used to monitor the microwave properties of a sample using an EMP. As can be seen in Fig. 3b, one can fix the operation frequency at f_x and monitor the change in the reflection amplitude. f_x is usually chosen to yield maximum change in the probe's reflection coefficient for a given range of parameters in a sample.

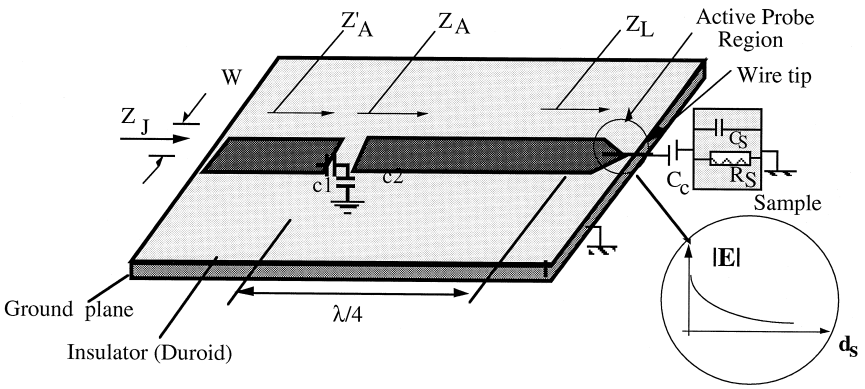
Z'A
ZA
ZL
Active Probe Region
W
Wire tip
ZJ
c1
c2
Cc
Cs
Rs
Sample
|E|
Ground plane
λ/4
Insulator (Duroid)
ds

(a)

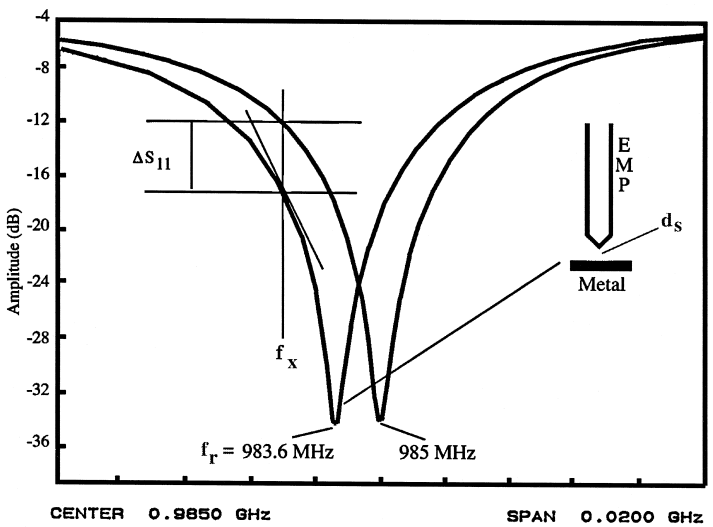
-4
-8
-12
-16
-20
-24
-28
-32
-36
Amplitude (dB)
ΔS11
fx
fr = 983.6 MHz
985 MHz
EMP
ds
Metal
CENTER 0.9850 GHz
SPAN 0.0200 GHz

(b)

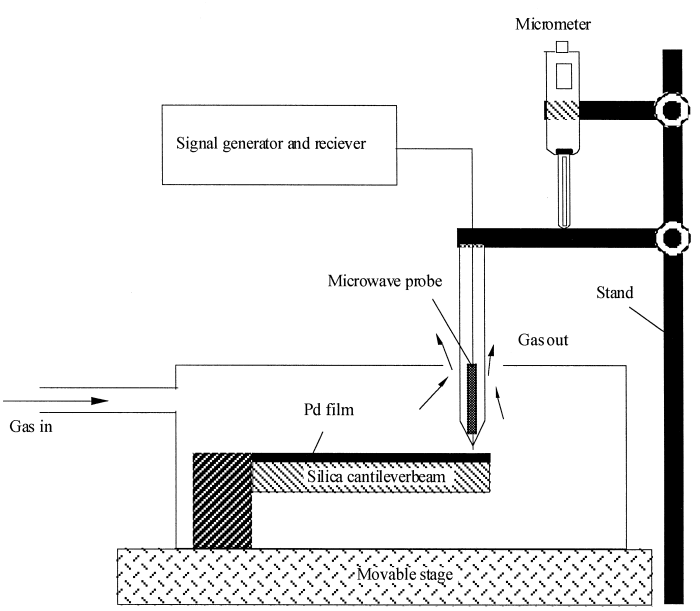
Micrometer
Signal generator and reciever
Microwave probe
Stand
Gas out
Gas in
Pd film
Silica cantileverbeam
Movable stage

(c)

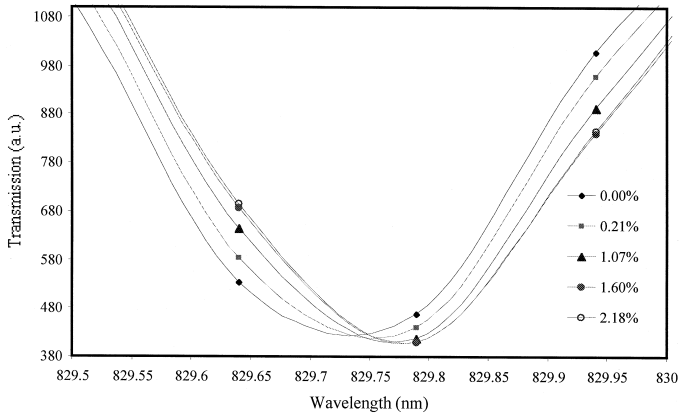

Fig. 4. Transmission spectrum of the FBG sensor as a function of hydrogen concentrations. The sensor was coated with a 0.56-μm thick Pd.

To measure the beam deflection using the microwave probe, by using the set-up in Fig. 3c, the probe was scanned over the beam and the stage was then adjusted until the probe was perpendicular to the beam surface. The probe was then positioned above the end of the Pd-coated beam. Next, the probe output as a function of the probe-sample distance was calibrated by using a micrometer. Theoretically the probe output is sensitive to a change in the conductivity of the sample as well as the distance between the probe and the sample. However, it was found that the probe output was dominated and mainly sensitive to the physical change in the probe-sample distance. After the calibration, the probe-sample distance was kept unchanged at a fixed position throughout the entire experiment. When the Pd-coated beam was exposed to hydrogen, it bent downward indicating that the film volume was expanding due to the hydrogen absorption. To keep the probe-sample distance fixed, we monitored the EMP output and kept it at a constant value by lowering the EMP downward using a micrometer. This procedure enabled us to determine the amount of the bending that occurred in the Pd-coated cantilever beam just by reading the micrometer dial. Once the beam deflection was known, the stress was computed using the formula [12];

$$\sigma = \frac{Y}{6(1-\nu)} \frac{t^2}{b} \frac{d}{L^2} \qquad (2)$$

where t is the beam thickness, L is the beam length, d is the beam deflection and b is the Pd film thickness. Y and ν are Young's modulus and the Poisson ratio of glass substrate, respectively. In this work, the beam is made of a 0.15 mm × 0.5 cm × 2.0 cm cover glass.

3. Results and discussion

Transmission spectra of a sensor as a function of hydrogen concentration are shown in Fig. 4. The Bragg wavelength of this sensor was 829.73 nm and it had a 35-μm cladding and a 560-nm Pd coating. From the figure, the Bragg wavelengths of the sensors were shifted to the right when the sensor was exposed to a higher hydrogen concentration. The sensor showed a completely reversible response to cycles of hydrogen/nitrogen exposures at low hydrogen concentrations. However when exposed to hydrogen concentrations higher than 1.8%, the Pd coating peeled off and the sensor was destroyed. This problem could be solved by adding a thin adhesion layer such as Ni [4] or Ti [6] to improve adhesion between the Pd and the fiber.

Fig. 5 shows the hydrogen sensitivity of the sensor. The Bragg wavelength increased almost linearly as a function of hydrogen concentrations in the range of 0.3–1.8% H_2 and decreased and became irreversible when it was exposed to hydrogen above 1.8%. Optical pictures of the sensors after exposure to 1.8% H_2 revealed that the Pd coating peeled off. In the linear range of its operation, the sensor had 1.95×10^{-2} nm/1% H_2 sensitivity.

Fig. 6 shows the spectrum from an array of two sensors with the Bragg wavelengths at 829.73 and 846.65 nm. These sensors were jointed together using a mechanical splicer. In Fig. 6, the top curve shows the transmission spectrum from the array of the two sensors in which only the second sensor was exposed to hydrogen (1% in nitrogen ambient). The second sensor clearly responded to hydrogen, as indicate in the bottom curve in the figure

Fig. 3. Schematic of the set-up for measuring stress in Pd thin films using a cantilever beam. (a) The EMP. (b) The reflection coefficient of EMP when an object is placed near the probe. (c) The apparatus that was used to measure the deflection of the Pd-coated cantilever beam using the EMP.

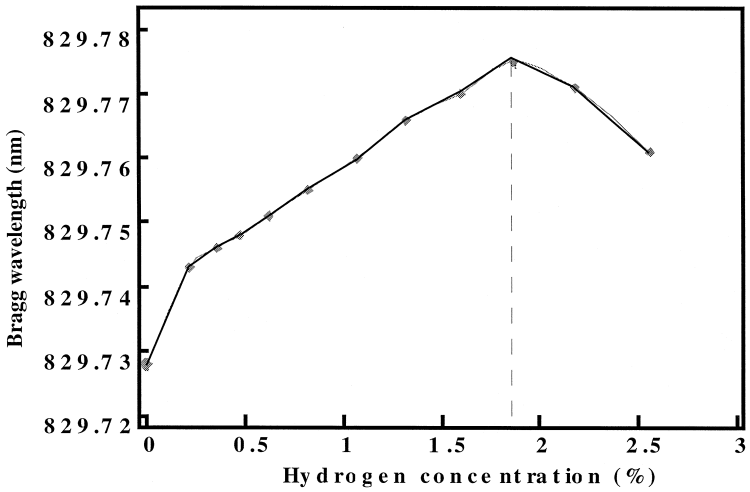

Fig. 5. Bragg wavelengths of the FBG sensor as a function of hydrogen concentrations. After exposure to 1.8% H_2, the sensor response deteriorated and became irreversible.

which shows the difference between the spectrum with and without hydrogen.

Using the apparatus shown in Fig. 3, we were able to determine hydrogen induced stress in the Pd film. Table 1 lists the beam deflections as a function of hydrogen concentrations and the calculated stress using the Eq. (2). The following parameters were used: $t = 50$ nm, $L = 2.0$ cm, $Y = 7.3 \times 10^{10}$ Pa and $\nu = 0.22$. The corresponding strain in the Pd film was calculated by using a well-known stress–strain relationship, i.e., $\varepsilon = \sigma/Y$. The Pd film was exposed to hydrogen concentrations below 1.5%, keeping the film from peeling off the substrate and blistering.

The stress in the Pd film was about three times higher than that found in the bulk Pd. The data suggests that there is higher hydrogen content in the thin film form (amorphous) than in the bulk (single crystal). The enhanced hydrogen solubility of the Pd film may occur at the grain boundaries as well as the air/Pd interface, producing strain variation across the film thickness.

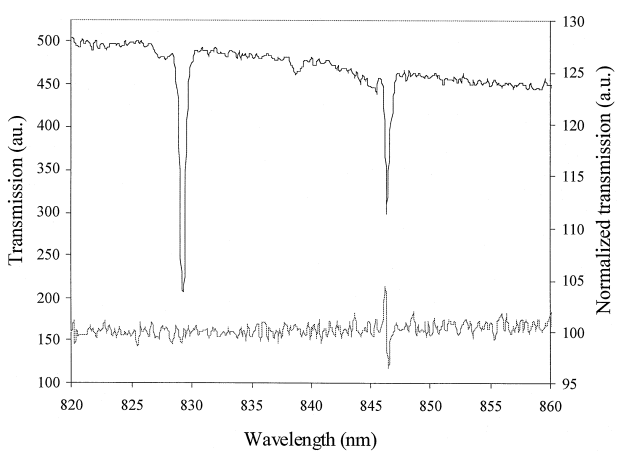

Fig. 6. Transmission spectrum of the two multiplexed FBG sensors (top) where only the second sensor was exposed to 1% H_2. The bottom curve is the difference between the sensors' spectra with and without (the reference spectrum) the hydrogen exposure.

4. Sensor modeling

Qualitatively we can use Eq. (1) to explain the sensor behavior when it is subjected to the changes in hydrogen concentration and in temperature. When the sensor is exposed to hydrogen, the grating period of the sensor increases due to the expansion of the palladium coating. In similar fashion, the grating period is also affected by the changes in the ambient temperature as a result of thermal expansion or contraction of the palladium coating. In addition, the effective refractive index of the silica fiber itself is temperature dependent. According to Eq. (1), the Bragg wavelength should increase when the sensor is exposed to higher hydrogen concentrations or temperatures because of the expansion of the grating and the increase of the effective refractive index of the fiber.

For quantitative analysis, we use the model proposed by Butler and Ginley [6] to determine the axial strain in the fiber core. In their work, the authors assumed that the relationship between the hydrogen content inside the bulk palladium and the partial pressure of hydrogen gas outside the bulk follows Sievert's law [13]. They used this information to calculate the fractional change in the dimensions (or strain) of the palladium coating. In this work, we determine the sensor response to hydrogen and temperature separately.

4.1. Sensor response to hydrogen

The shift in Bragg wavelength with strain can be expressed using [9]

$$\Delta\lambda_B = 2n_{\text{eff}}\Lambda\varepsilon\left[1 - \left(\frac{n_{\text{eff}}^2}{2}\right)\left[P_{12} - \nu(P_{11} + P_{12})\right]\right] \quad (3)$$

Table 1
Deflections (d) of the Pd-coated cantilever beam and calculated stress (from Eq. (2)) and strain ($\varepsilon = \sigma/Y$) in the Pd film as a function of hydrogen concentrations
The strain of a bulk Pd is also given.

H_2 Concentration (%)	Deflection, d (μm)	Stress, σ (Pa)	Strain ($\varepsilon = \sigma/Y$)	Strain in bulk Pd ($\varepsilon = 0.26p^{1/2}/K$)
0.49	3.0	5.26×10^7	4.34×10^{-4}	1.43×10^{-4}
0.80	3.9	6.84×10^7	5.65×10^{-4}	1.83×10^{-4}
1.07	4.5	7.90×10^7	6.53×10^{-4}	2.11×10^{-4}
1.41	4.9	8.59×10^7	7.85×10^{-4}	2.43×10^{-4}

where ε is the applied strain, P_{11} and P_{12} are the Pockel's coefficients of the strain-optic tensor, ν is the Poisson's ratio. For a typical silica fiber, $P_{11} = 0.113$, $P_{12} = 0.252$, $\nu = 0.16$, and $n = 1.482$. Using these parameters, the above expression is simplified to

$$\frac{\Delta\lambda_B}{\varepsilon\lambda_B} = 0.78 \times 10^{-6}\mu\varepsilon^{-1} \quad (4)$$

where λ_B is the Bragg wavelength of the FBG at zero applied strain. For $\lambda_B = 1.3$ μm, the wavelength shifts 1 nm per 1000 micro-strain.

As Pd absorbs hydrogen, it expands, producing stress (strain) in the bulk materials. Strain in a free-standing bulk Pd is equal to the ratio of the fractional change in the lattice constant of the Pd. In the α-phase, the relationship between the strain of Pd and the hydrogen content is given by [6]

$$\delta = 0.026x \quad (5)$$

where x is the hydrogen content of the palladium. The relationship between the hydrogen content and the partial pressure of hydrogen gas in the α-phase follows Sievert's law [13]:

$$p^{1/2} = Kx \quad (6)$$

where p is the hydrogen partial pressure (Torr) and K is the Sievert's coefficient ($K = 350$ Torr$^{1/2}$). Combining Eqs. (5) and (6), we obtain the strain as a function of partial pressure of hydrogen gas:

$$\delta = 0.026\frac{\sqrt{p}}{K} \quad (7)$$

The next step is to calculate the strain in the FBG core due to an expansion of the Pd coating. For simplicity, we consider only the axial strain. The force acting on the FBG due to the Pd expansion is $\delta Y_{Pd} A_{Pd}$ and the force acting on the coating is $\varepsilon_F(Y_F A_F + Y_{Pd} A_{Pd})$. Here, Y is Young's modulus and A is the area. By balancing the two forces, we get the axial strain in the FBG:

$$\varepsilon_F = \delta\frac{(b^2 - a^2)Y_{Pd}}{a^2 Y_F + (b^2 - a^2)Y_{Pd}} \quad (8)$$

where a and b are the cladding and total sensor diameters, respectively (see Fig. 1), and Y_{Pd} and Y_F are Young's moduli of palladium and silica fiber.

The shifts in Bragg wavelengths of the Pd-coated FBGs as a function of hydrogen partial pressure can be obtained by substituting the axial strain in Eq. (8) into Eq. (2):

$$\Delta\lambda_B = \frac{0.026\sqrt{p}}{k}\left[\frac{(b^2 - a^2)Y_{Pd}}{a^2 Y_F + (b^2 - a^2)Y_{Pd}}\right] \times 0.78\lambda_B \quad (9)$$

Here, the hydrogen partial pressure has a unit of Torr. Fig. 7 shows the Bragg wavelengths calculated by using Eq. (9), curve (a). This sensor has a cladding diameter of 35 μm and a Pd film thickness of 0.56 μm. For curve (b), Bragg wavelengths were calculated in the same manner as in curve (a) but the measured film stress was taken from Table 1 instead of the bulk stress. Both curves show that the sensor has a linear response to hydrogen in the range 0.3–1.8% H_2. The linear relationship is also found in the experimental values as can be seen in curve (c).

4.2. Response to temperature

The shift in Bragg wavelength of a Pd-coated FBG with temperature is contributed by two components: the thermal effects on the optical fiber itself and the stress due to thermal expansion of the Pd coating. The thermal effect on the optical fiber is well-known and well-characterized [9]. This thermal response of the fiber arises due to the inherent thermal expansion of the fiber material and the thermo-optic effect in which the index of refraction of the

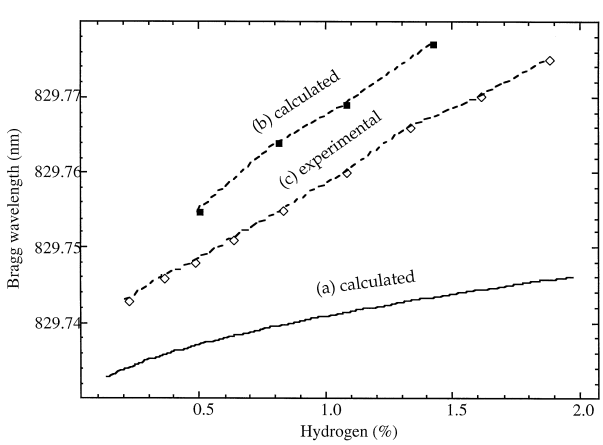

Fig. 7. Hydrogen sensitivities of the FBG sensor. (a) Calculated by using Eq. (9), (b) calculated by using Eq. (9) but using measured strain shown in Table 1, and (c) the experimental results. The sensor had a 35-μm thick cladding and 0.56-μm thick Pd coating.

fiber changes with temperature. The thermal response of the FBGs is found to be given by [9]

$$\Delta\lambda_B = \left[\alpha_F + \left(\frac{1}{n}\right)\frac{dn}{dT}\right]\Delta T\lambda_B = 6.67\times10^{-6}\Delta T\lambda_B{}^{\circ}C^{-1} \quad (10)$$

where α_F is the coefficient of thermal expansion of the silica fiber. The term dn/dT, representing the temperature dependence of the fiber's refractive index accounts for about 95% of the wavelength shift. The wavelength shifts by ≈ 0.1 nm per temperature increment of 10°C at $\lambda_B = 1.3$ μm.

When the temperature changes, both the fiber and the Pd coating expand. The effect of the thermal-induced expansion of the Pd coating to the Bragg wavelength behaves similarly to the response of the Pd-coated FBG to hydrogen as previously described. The thermal expansion coefficient of palladium is $11\times10^{-6}/°C$ at 20°C which is much higher than the $0.55\times10^{-6}/°C$ of the silica fiber. As temperature changes, the higher rate of expansion or contraction of the Pd coating will either strain or compress the FBG, resulting in the change in the grating period. The shift of Bragg wavelength as a function of temperature induced by the coating is the same as the shifts due to the hydrogen absorption by the film. The stress due to hydrogen absorption is replaced by the thermal stress as follows

$$\Delta\lambda_B = \left[\frac{(b^2-a^2)Y_{Pd}}{a^2Y_{cl}+(b^2-a^2)Y_{Pd}}\right]\alpha_{Pd}\Delta T\lambda_B \quad (11)$$

Using the same sensor parameters as in Fig. 5 (35-μm thick cladding and 0.56-μm thick Pd coating) the wavelength shift calculated from Eqs. (10) and (11) are 5.53×10^{-3} and 0.89×10^{-3} nm/°C, respectively, at 20°C and $\lambda_B = 829.73$ nm. Thus, the total shift due to temperature is 6.42×10^{-3} nm/°C. Therefore, this sensor has a combined hydrogen-temperature sensitivity of $0.33\%/H_2/°C$.

Higher hydrogen sensitivity could be achieved by increasing the thickness of the Pd coating or reducing the fiber cladding size as indicated in Eq. (9). However, this will increase the temperature sensitivity of the sensor and some optimization is required. We note that a fiber with a cladding smaller than 30–40 μm is very fragile and not practical. However, for thinner fiber claddings, it is also possible to take advantage of evanescent field interactions to enhance the sensor's hydrogen sensitivity as discussed in Ref. [14].

5. Conclusions

In conclusion, we have demonstrated a new type of hydrogen sensor that is based on the elastooptic effect in a fiber Bragg grating coated with Pd. This type of sensors allows several sensors to be easily multiplexed on one single fiber using simple and low-cost detection equipment. The sensor showed a linear sensitivity for 0.3–1.8% H_2. Stress in the Pd film as a function of hydrogen concentrations was also measured. The film stress was found to be about three times higher than the bulk values.

The long-term stability and temperature dependence of the sensors are currently being investigated. Minimum detectable resolution of the hydrogen concentration of the device is primarily limited by two factors: the resolution of the detecting equipment and the thermal stress caused by the Pd coating. The latter can be evaluated by comparing thermal stress to hydrogen absorption induced stress of the Pd coating and will be published in the future. The concept of using FBGs for measuring stress in the sensitive materials could be applied to other types of chemicals and gases as well as to in situ stress measurements in thin films during the course of the deposition.

References

[1] A.D. Kersey, A review of recent developments in fiber optic sensor technology, Opt. Fiber Technol. 2 (1996) 291–317.
[2] M. Tabib-Azar, Integrated Optics and Microstructure Sensors, Kluwer Academic Publishers, Boston, 1995, and references therein.
[3] G. Boisde, A. Harmer, Chemical and Biochemical Sensing with Optical Fibers and Waveguides, Artech House, Boston, 1996, and references therein.
[4] M.A. Butler, Micromirror optical-fiber hydrogen sensor, Sens. Actuators, B 22 (1994) 155–163.
[5] M.A. Butler, Fiber optic sensor for hydrogen concentration near the explosive limit, J. Electrochem. Soc. 138 (1991) 46–47.
[6] M.A. Butler, D.S. Ginley, Hydrogen sensing with palladium-coated optical fibers, J. Appl. Phys. 64 (1988) 3706–3711.
[7] K.O. Hill, G. Meltz, Fiber Bragg gratings technology fundamentals and overview, J. Lightwave Technol. 15 (1997) 1263–1276.
[8] A. Othonos, Fiber Bragg gratings, Rev. Sci. Instrum. 68 (1997) 4309–4341.
[9] A.D. Kersay, M.A. Davis, H.J. Patrick, M.L. LeBlanc, K.P. Koo, C.G. Askins, M.A. Putnam, E.J. Friebele, Fiber grating sensors, J. Lightwave Technol. 3 (1997) 1442–1462.
[10] Y.J. ao, In-fibre Bragg grating sensors, Meas. Sci. Technol. 8 (1997) 355–375.
[11] D.P. Su, A. Pohar, M. Tabib-Azar, 0.4 μm Spatial resolution with 1 GHz evanescent microwave probe, Rev. Sci. Instrum., March 1999.
[12] D.S. Campbell, 1970, in: L.I. Maissel, R. Glang (Eds.), Handbook of Thin Film Technology, Vol. 12, McGraw-Hill, New York, pp. 21–50.
[13] F.A. Lewis, The Palladium Hydrogen System. Academic Press, London, 1967.
[14] M. Tabib-Azar, B. Satupan, R. Petrick, A. Kazemi, Highly sensitive hydrogen sensors using palladium coated fiber optics with exposed cores and evanescent field interactions, Sens. Actuators (1999) in press.